Structure of High-Temperature $NaF-AlF_3-Al_2O_3$ Melts: A Multinuclear NMR Study

Vincent Lacassagne,[†] Catherine Bessada,*[,†] Pierre Florian,[†] Sylvie Bouvet,[‡] Benoist Ollivier,[‡] Jean-Pierre Coutures,[†] and Dominique Massiot[†]

Centre de Recherche sur les Matériaux à Haute Température, CRMHT-CNRS, 1D avenue de la Recherche Scientifique, 45071 Orléans Cedex 2, France, and CRV Pechiney, BP 27, 38340 Voreppe, France

Received: August 10, 2001; In Final Form: November 29, 2001

Fluoroaluminate molten salts are used in the Hall-Heroult industrial process for the production of aluminum by electrolysis. To better understand the mechanism of the dissolution of alumina (Al_2O_3) in cryolitic melts, we have studied the structure of these liquids up to 1025 °C by in-situ NMR of ^{27}Al, ^{23}Na, ^{19}F, and ^{17}O, using a laser-heated experimental setup. From these experiments we can propose a quantification of the different aluminum-bearing species AlF_4^-, AlF_5^{2-}, and AlF_6^{3-} in the liquid and give a direct experimental evidence of the existence of at least two different oxy-fluoride species, $Al_2OF_6^{2-}$ and $Al_2O_2F_4^{2-}$, when dissolving alumina in the fluoride liquid. The obtained results are compared with other spectroscopic data obtained by in-situ Raman spectroscopy.

1. Introduction

Cryolitic liquids ($NaF-AlF_3$ binary system) with dissolved aluminum oxide (Al_2O_3) are used for the production of metallic aluminum by the Hall-Heroult electrolytic process.[1] These corrosive and experimentally difficult-to-handle liquids have been the subject of numerous studies including experimental (density, viscosity, electrical conductivity) approach and modeling.[1] More recently Raman[2−4] and NMR[5−8] spectroscopies, with in-situ studies at high temperature, have been used experimentally to better describe the structure of the cryolitic liquids and compare the experimental point of view to results obtained from thermodynamical[9−15] or computational modeling.[16−22] Gilbert et al.[2] have extensively studied the structure of fluoroaluminate molten salts and proposed a quantitative description of the melt in terms of ionic complexes. The model described by these authors combines results from Raman spectroscopy and thermodynamics data, and involves three fluoroaluminate species AlF_4^-, AlF_5^{2-}, and AlF_6^{3-} together with free fluorine. However the existence of major amounts of AlF_5^{2-} remains a subject of a number of discussions.

In alkali fluoroaluminate solid compounds, aluminum is present only in octahedral coordination with fluorine. Their ^{27}Al chemical shifts range between −13 and +1.4 ppm and are typically more shielded than the AlO_6 octahedra in oxide compounds.[23−27] Only a few studies report lower coordination numbers for Al in fluorides: Kohn et al.[26] have described the ^{27}Al MAS NMR spectra of glasses of jadeite mixed with cryolite, in terms of Al_V and Al_{VI} coordination at 22 and −5 ppm, respectively; Herron et al.[28] reported a ^{27}Al chemical shift at 49 ppm for the tetrahedral anion AlF_4^- in a [1,8-bis-(dimethylamino)naphthaleneH$^+$] [AlF_4^-] saturated solution.

In these liquids, for all the observed nuclei, the high-temperature NMR spectrum consists, in a single, narrow line, characterized by its position (isotropic chemical shift) and its line width. This single sharp line reflects rapid exchange between the different available environment, (rapid as compared to NMR time scales ranging from 10^2 to 10^8 Hz). Consequently, the observed peak position is the average of the chemical shifts of individual species, weighted by their respective populations. In a pioneering high-temperature NMR study, Stebbins et al.[5] reported ^{27}Al chemical shifts for four compositions of the $NaF-AlF_3-Al_2O_3$ system that were systematically much higher in the liquid than in the related solid phases. They emphasized the *dramatic* effect of composition and temperature on the liquid structure and proposed an evolution of aluminum environment toward a higher fraction of 4-fold coordinated environments of aluminum. Using the laser-heated NMR setup developed in Orleans,[29] we studied the ^{27}Al NMR signature for a wider range of high-temperature liquid compositions of the $NaF-AlF_3$ system and compared the obtained results to existing Raman data,[7] showing that both spectroscopies quantitatively agreed in describing the structure of the liquid phase in terms of AlF_4, AlF_5, and AlF_6 ionic complexes. We also reported well-separated ^{27}Al chemical shifts ranges for the different types of aluminum coordinations in fluoroaluminates,[8] including the AlF_4 coordination, measured at 38 ppm on the high-temperature NMR spectrum of the $NaAlF_4$ melt where Raman spectroscopy gave evidence of only AlF_4^- species.(Table 1).

The aim of this contribution is to present new results obtained by a multinuclear (^{19}F, ^{27}Al, and ^{23}Na) NMR study of the high-temperature liquids of the $NaF-AlF_3$ binary systems and to discuss the mechanism of dissolution of alumina (Al_2O_3) in cryolite-based liquids from the observation of ^{17}O. Due to its high polarizability ^{17}O has a large range of chemical shifts and is thus very sensitive to the structure of its local environment in crystalline, amorphous, or liquid materials.[30−32] Its observability is limited only by its very low intrinsic sensitivity due to low natural abundance (0.037%) that can be circumvented by isotopic enrichment. The combination of information obtained from the observation by NMR of all the different nuclei present in these high-temperature melts enables us to discuss previously proposed models of the liquid structure and to give the first experimental evidence of the presence of at least two oxyfluoride species upon dissolution of alumina.

* Corresponding author. Fax: +33(0) 238 638 103. E-mail: bessada@cnrs-orleans.fr.
[†] CRMHT-CNRS.
[‡] CRV Pechiney.

10.1021/jp013114l CCC: $22.00
Published on Web 02/02/2002

TABLE 1: ^{27}Al Chemical Shifts Values for Al−O and Al−F Coordination[8]

aluminum coordination	δ^{Al} (ppm)
AlO_4^{5-}	90/55
AlO_5^{7-}	30/40
AlO_6^{9-}	20/−20
AlF_4^-	38
AlF_5^{2-}	20
AlF_6^{3-}	1.4/−13

2. Experimental Section

Samples have been prepared in a glovebox under an argon atmosphere by mixing suitable proportions of natural cryolite (from Ivigtut), AlF_3 (Inland, 99.9% purified by two sublimations at 1000 °C), NaF (Aldrich, 99.9%), and α-Al_2O_3 (APA 05). The ^{17}O-enriched alumina has been synthesized in the laboratory from 46% ^{17}O-enriched H_2O and aluminum isopropoxide. Samples were preheated in a furnace at 1025 °C under argon before NMR experiment. Weight losses were checked to be always less than 2%.

In the binary $NaF-AlF_3$ system we have investigated a composition range extending from 20 to 50% mol of AlF_3 and the NaF end member. AlF_3, the second end member of this binary diagram, sublimates before melting.

Mixtures of cryolite and ^{17}O-enriched Al_2O_3 (0.6 to 8.2 mol % of Al_2O_3) cover the whole range of alumina solubility in cryolite (up to 6 mol %) and the beginning of the saturation domain.

The high-temperature NMR experiments have been acquired using the previously described high-temperature laser-heated system[29,33−35] developed at CRMHT Orléans (France). The sample is contained in a high-purity boron nitride (BN AX05 Carborundum) crucible, tightly closed by a screwed BN cap, and put inside the RF coil, at the magnetic center of the cryomagnet. The NMR axial saddle coil is thermally isolated by a ceramic shield. The crucible is directly heated by a continuous CO_2 laser ($\lambda = 10.6$ μm) passing axially through the probe-head. With this design, temperature cannot be measured by a thermocouple during NMR experiments. The temperature calibration is carried out in two steps: calibration of temperature versus laser power using a thermocouple located inside the BN crucible controlled by in-situ observation of phase transitions by NMR. The $\alpha \rightarrow \beta$ transition and melting in cryolite are clearly marked by a net ^{27}Al signal modification. Respecting the same heating and cooling procedure, the temperatures reported below are accurate within ±5 °C. As liquid fluoride melts are very corrosive and subject to non congruent vaporization, the experimental time spent in the liquid phase has been minimized (≈5 min) to avoid evolution of the composition during the experiment. The chemical compositions of the samples were obtained by wet chemical analysis and cross checked by high-resolution NMR and Rietveld analysis of their X-ray diffraction patterns before and after high-temperature NMR experiments. Weight loss measurements confirmed the absence of evaporation out of the crucible.

All the NMR experiments have been carried out using a Bruker DSX400 NMR spectrometer operating at 9.4 T. The NMR spectra have been acquired using single pulse excitation, and typical acquisition conditions are reported in Table 2. ^{27}Al, ^{23}Na, ^{19}F, and ^{17}O chemical shifts are referenced to 1 M aqueous solutions $Al(NO_3)_3$, NaCl, $CFCl_3$, and H_2O, respectively, at room temperature, and are accurate to ±0.5 ppm. The reported ^{19}F spectra are corrected from a broad probe-head signal due to the presence of Teflon in the probe assembly.

TABLE 2: Typical Acquisition Conditions Used for High-Temperature NMR Experiments

nucleus	frequency (MHz) (9.4 T)	number of scans	pulse length (μs)	recycle delay (s)	reference
^{19}F	376.3	8	$\pi/2$	1	$CFCl_3$ 1 M
^{27}Al	104.2	64	$\pi/8$	0.5	$Al(NO_3)_3$ 1 M
^{23}Na	105.8	64	$\pi/8$	0.5	NaCl 1 M
^{17}O	54.2	64	$\pi/2$	0.5	H_2O

^{27}Al, ^{23}Na, and ^{19}F solid-state MAS NMR spectra have also been performed at room temperature on stable compounds of the system $NaF-AlF_3$, to correlate the experimental chemical shifts and the structural features given by crystallographic data. The solid-state NMR data were collected with the same spectrometer (9.4 T) using a 4 mm double bearing MAS probe from Bruker for a 15 kHz spinning rate. The acquisition parameters were chosen to optimize the resolution: short pulse lengths (0.5 μs), recycle times of 1 to 5 s, and a high number of scans (1024). We have reported in Table 3, the correspondence between experimental NMR chemical shifts and coordination for a given nucleus.

For the ^{17}O, the chemical shifts reported by Walter et al.[30] for OAl_4^{10+} sites in the different types of alumina ($\delta,\theta,\eta,\alpha$) lie between 72 and 75 ppm. It should be noticed that due to its high quadrupolar coupling ($C_Q \approx 1.5-2$ MHz), and its low amount in the baths, the ^{17}O signal will be visible in our experimental conditions only when involved in the liquid phase.

3. Results and Discussion

3.1. $NaF-AlF_3$. ^{27}Al, ^{23}Na, ^{19}F NMR spectra of the different melts consist in a single Lorentzian line, characteristic of rapid exchange between the different chemical species in the liquid. The typical line widths of the lines are constant, of the order of 100 to 200 Hz, and mainly due to principal field inhomogeneity as could be checked by relaxation time measurements.

We have reported in Figure 1 the evolution of ^{27}Al, ^{23}Na, and ^{19}F chemical shifts over the composition range, between 20 and 50 mol % of AlF_3, with the ^{23}Na and ^{19}F chemical shifts measured in pure liquid NaF. Going from NaF to AlF_3 we observe a continuous decrease, respectively increase, of $\delta_{^{23}Na}$ and $\delta_{^{27}Al}$. In both cases we notice a change of slope between the compositions of chiolite ($Na_5Al_3F_{14}$) and cryolite (Na_3AlF_6). In contrast with ^{27}Al and ^{23}Na the position of the ^{19}F line rapidly grows from liquid NaF ($\delta = -228$ ppm), stabilizes between chiolite and cryolite at ≈ −192 ppm, and lowers for higher contents of AlF_3.

As already described in a preceding paper,[7] from the evolution of the ^{27}Al chemical shift it is clear that the ionic structure of these melts consists of more than one type of aluminum-containing ionic species, the proportion of which depends on the composition. From the knowledge of the whole chemical shift range for 6-fold aluminum coordinated with F, and the 38 ppm value measured for AlF_4^- complexes, it turns down all the structural description involving only AlF_6^{3-} ionic species, even as distorted AlF_6^{3-} complexes.[12,13,15,18] For a dissociation scheme involving only AlF_4^- and AlF_6^{3-}, the distribution of these two ionic species calculated directly from the experimental NMR chemical shifts for the different compositions would not coincide with any models previously described.[14] Between chiolite and cryolite cryolitic ratio, the anionic molar fractions calculated for AlF_4^- and AlF_6^{3-} species would be nearly identical and follow the same decreasing trend, while the calculated equilibrium constant varies of 1 order of magnitude (0.02 to 0.21 at 1025 °C) over the whole range of AlF_3 content.

TABLE 3: Coordination and Experimental Chemical Shifts for Sodium and Aluminum Fluoride Solid Stable Phases

		δ^{27}Al (ppm)					δ^{23}Na (ppm)					δ^{19}F (ppm)	
compound	site	(*a*)	(*b*)	(*c*)	compound	site	(*a*)	(*b*)	(*c*)	compound	site	(*a*)	(*d*)
AlF_3	AlF_6^{3-}	−15	−13.2		NaF	NaF_6^{5-}	7	7.2		NaF	FNa_6^{5+}	−221	
Na_3AlF_6	AlF_6^{3-}	−1	1.4	0	Na_3AlF_6	NaF_6^{5-}	1	2.4	4	Na_3AlF_6	FNa_3Al^{5+}	−189	
$Na_5Al_3F_{14}$	AlF_6^{3-}	−1.5	−1	−1	Na_3AlF_6	NaF_8^{7-}	−12	−9.3	−8	$Na_5Al_3F_{14}$	FNa_3Al^{5+}	−187	−189.5
$Na_5Al_3F_{14}$	AlF_6^{3-}	−2.8	−3	−3	$Na_5Al_3F_{14}$	NaF_6^{5-}	−7		−6	$Na_5Al_3F_{14}$	FNa_4Al^{6+}	−190	−191.4
$NaAlF_4$ (molten)	AlF_4^-	38			$Na_5Al_3F_{14}$	NaF_{12}^{11-}	−21		−21	$Na_5Al_3F_{14}$	FAl_2^{5+}	−162	−165

[a] This study. [b] Ref 24. [c] Ref 5. [d] Ref 36.

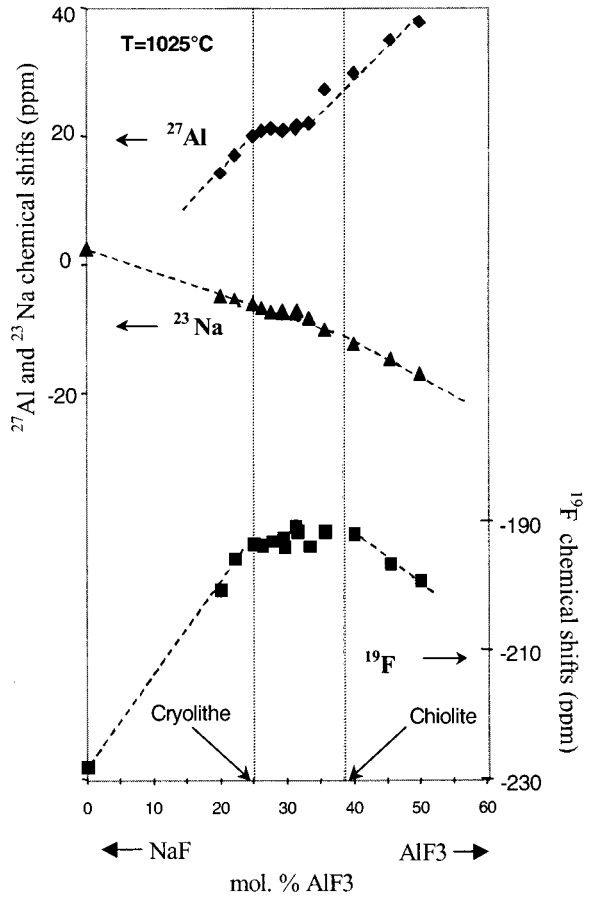

Figure 1. ^{19}F, ^{23}Na, and ^{27}Al chemical shifts in cryolitic melts at 1025 °C.

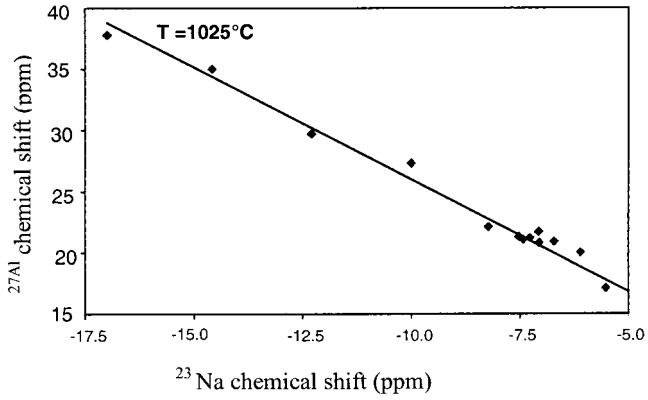

Figure 2. Linear correspondence between ^{27}Al and ^{23}Na chemical shifts measured over the whole range of compositions.

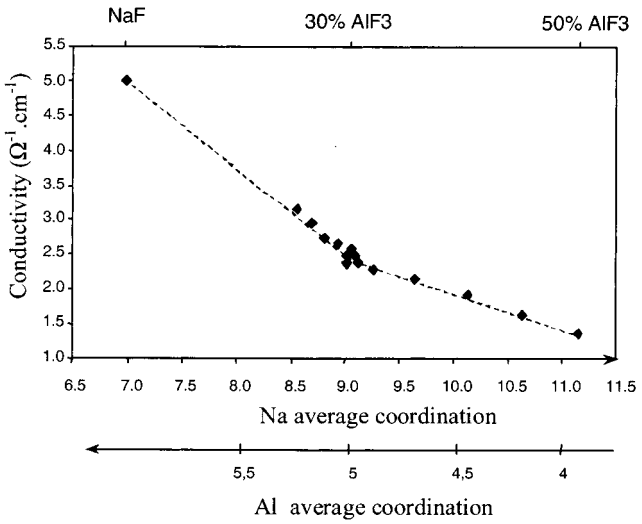

Figure 3. Conductivity data[1] reported vs Al and Na average coordination.

We can describe the observed chemical shifts in terms of structural environment of the observed nucleus, by using the correspondence between experimental chemical shifts and coordination, described in Table 3 and established at room temperature for solid stable compounds. From 18 to 50% AlF_3, the averaged coordination number of aluminum with fluorine decreases from 5.5 to 4 and that of sodium increases from 8.5 to 11. The correlation between chemicals shifts of ^{23}Na and ^{27}Al is equivalent to a correlation between averaged coordination numbers, which indicates that these melts can be described from the Al−F as from the Na−F point of view.

It is interesting to notice that the observed singularity in both the aluminum and sodium observed chemical shift closely corresponds to behavior already observed for macroscopic properties such as conductivity, density, and viscosity.[1] We have correlated the conductivity data measured in liquids of the binary $NaF-AlF_3$ system, with the average coordination evolution of Na and Al atoms deduced from our high-temperature NMR data (Figure 3). The conductivity decreases rapidly with increasing the amount of AlF_3 in the melt, and coincides rather well with the coordination evolutions, respectively, increasing for Na and decreasing for Al. A modification in this evolution is evidenced around 30 mol % AlF_3 by a break of the slope. According to the Raman description of such melts, this particular composition corresponds to that with the minor amount of free fluorine, the major fraction of AlF_5^{2-}, and the emergence of AlF_4^-. This observation confirms the high relation between the macroscopic properties and the liquid microstructure in terms of anionic species and their relative proportions.

To better describe the ^{19}F chemical shifts evolution, we need some additional information. In the dissociation scheme of the cryolitic melts, fluorine is involved in four possible different species: AlF_4^-, AlF_5^{2-}, AlF_6^{3-}, and F^-. From the anionic proportions reported by Gilbert et al.,[2] we can calculate the atomic fraction of fluorine inside each of these species.

Moreover, the ^{19}F chemical shift of individual fluoroaluminate anion can be directly deduced from our experimental data. The value measured in pure molten NaF at −228 ppm is assigned

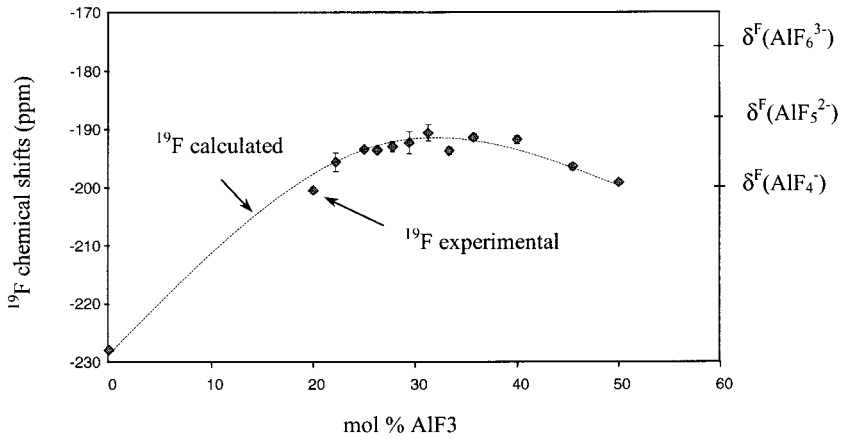

Figure 4. ^{19}F chemical shifts: experimental and calculated from the anionic fractions reported by Gilbert et al.[2]

to the free fluorine ion. For the melt of $NaAlF_4$ composition (50 mol % AlF_3) where F^- is involved only in AlF_4^-, the ^{19}F chemical shift is measured at -200 ppm (δ^F_{IV}). The chemical shift evolution has been fitted over the whole range of composition (Figure 4), and we find a really satisfying modeling with $\delta^F_V = -188$ ppm and $\delta^F_{VI} = -176$ ppm. These results show the strong dependence of ^{19}F chemical shifts with the amounts of free fluorine ions in the melts: the increase in chemical shift between 0 and 25 mol % AlF_3 can be correlated with the decrease of the anionic fraction of F^- ion.

Thus, the interpretation of both ^{27}Al and ^{19}F chemical shifts variations in terms of fluoroaluminate species confirm the coherence of such a description in cryolitic melts.

3.2. $NaF-AlF_3-Al_2O_3$. The NMR spectra obtained for the four nuclei of the system, ^{27}Al, ^{23}Na, ^{19}F, and ^{17}O, are reported on Figure 5 for the different Al_2O_3 additions (0.6 to 8.2 mol %).

Except for aluminum spectra where broadening of the lines is observed with increase of the dissolved amount of alumina, for the other nuclei, the evolution of the line width is not significant.

A small, but significant ^{17}O signal is observed from 0.6 mol % Al_2O_3. The intensity of the line increases with the amount of alumina dissolved and indicates the increase of the number of ^{17}O nuclei in the melt up to the maximum value at the melt saturation.

The ^{27}Al spectra show also a strong evolution with alumina addition, and shift toward higher chemical shifts. No significant evolution of ^{19}F and ^{23}Na signatures are observed and the chemical shifts appear rather constant over the whole range of compositions. In Figure 6, the chemical shift data are reported vs the mol % of Al_2O_3 for the four nuclei.

The evolutions observed for ^{17}O and ^{27}Al are nearly symmetrical except for the highest values of alumina content after which the chemical shifts are constant. These simultaneous evolutions indicate in the melt the existence of Al−O−F species, in addition to fluoroaluminate species already described for the $NaF-AlF_3$ binary system. The ^{27}Al chemical shifts increase from 20 to 47 ppm over the range 0 to 6.6 mol % alumina, and stay constant at 47 ppm for adding higher than 6.6%.This strong variation indicates that the average local environment of aluminum is highly modified by the addition of alumina. The chemical shift values become rapidly higher than 38 ppm, which is the maximum value measured in the binary system $NaF-AlF_3$ for AlF_4^-. It means that new chemical species with higher chemical shift are to be considered in the melt. The chemical shift remains constant above 6.6% and indicates the saturation of the melt, with alumina (beyond 6%).

The exact anionic structure of the oxyfluoride species is still a matter of controversy. A number a studies yet converge clearly toward two major entities containing oxygen, namely $Al_2OF_6^{2-}$ and $Al_2O_2F_4^{2-}$, where the former appears to be the dominating one at a low amount of alumina[4,14,20] while the other is the unique species for higher Al_2O_3 content.

The ^{17}O chemical shift decreases from 25 to 8.5 ppm, in the range of 0.6 to 3.8 mol % of alumina, and then remains constant above 3.8%. The high sensibility of the ^{17}O chemical shift with the added alumina content shows that the average local environment of oxygen atoms is strongly modified up to 3.8%. From these direct observations we can already propose from the evolution of the ^{17}O chemical shift that, in the melt up to 3.8 mol % Al_2O_3, more than one species exist, while above, the chemical shift being constant, we can suppose only one species exists. In the same manner, the variations of the ^{27}Al δ iso, up to the solubility limit, show that the alumina dissolution is always effective.

Oxygen atoms in these complexes are most probably involved in bridging bonds of the type Al−O−Al and

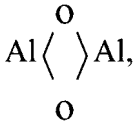

as it has been evidenced by Gilbert et al. from Raman spectroscopic measurements.[4] The chemical shifts evolution we have observed for the ^{17}O and ^{27}Al spectra really account for the existence of two different oxyfluoride species depending on the Al_2O_3 content. We have then based our description on the two species described above: at 0.6 mol % only the $Al_2OF_6^{2-}$ is present, while the $Al_2O_2F_4^{2-}$ appears to be the unique oxyfluoride for highest Al_2O_3 contents. We can extract then the corresponding chemical shifts values for each individual species as δ^o $Al_2OF_6^{2-} = 25$ ppm, and δ^o $Al_2O_2F_4^{2-} = 8.5$ ppm.

If we make the assumption that only these two species are present, the ^{17}O chemical shift, δ(O), can be expressed as

$$\delta(\mathrm{O}) = X^{\mathrm{O}}_{Al_2OF_6^{2-}}.\delta^{\mathrm{O}}_{Al_2OF_6^{2-}} + X^{\mathrm{O}}_{Al_2O_2F_4^{2-}}.\delta^{\mathrm{O}}_{Al_2O_2F_4^{2-}} \qquad (1)$$

with

$$X^{\mathrm{O}}_{Al_2OF_6^{2-}} + X^{\mathrm{O}}_{Al_2O_2F_4^{2-}} = 1 \qquad (2)$$

$X^{\mathrm{O}}_{Al_2OF_6^{2-}}$ and $X^{\mathrm{O}}_{Al_2O_2F_4^{2-}}$ are the atomic fractions of oxygen in $Al_2OF_6^{2-}$ and $Al_2O_2F_4^{2-}$, respectively.

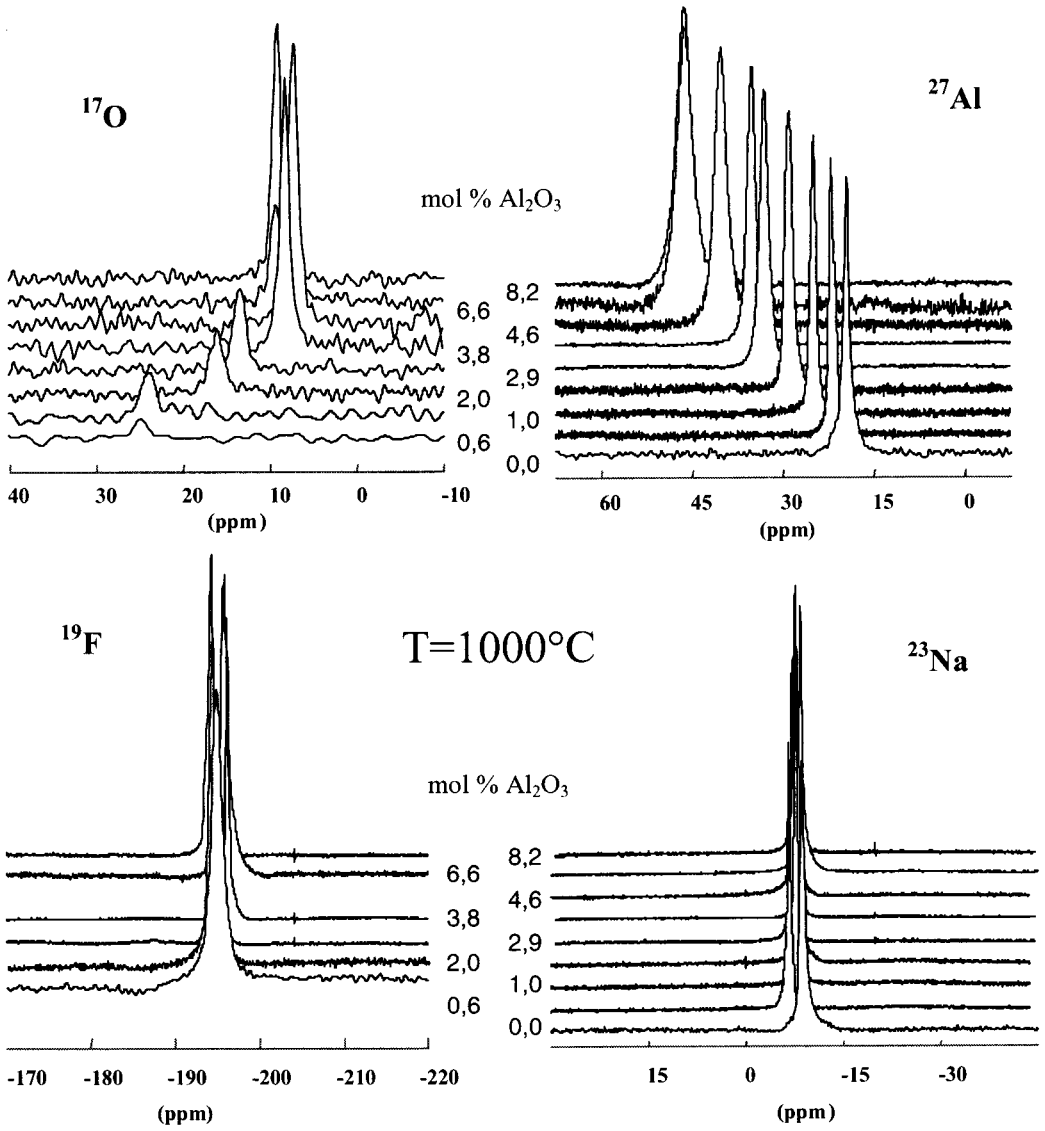

Figure 5. ^{17}O, ^{27}Al, ^{19}F, ^{23}Na spectra of ^{17}O-enriched alumina dissolution in cryolite at 1000 °C.

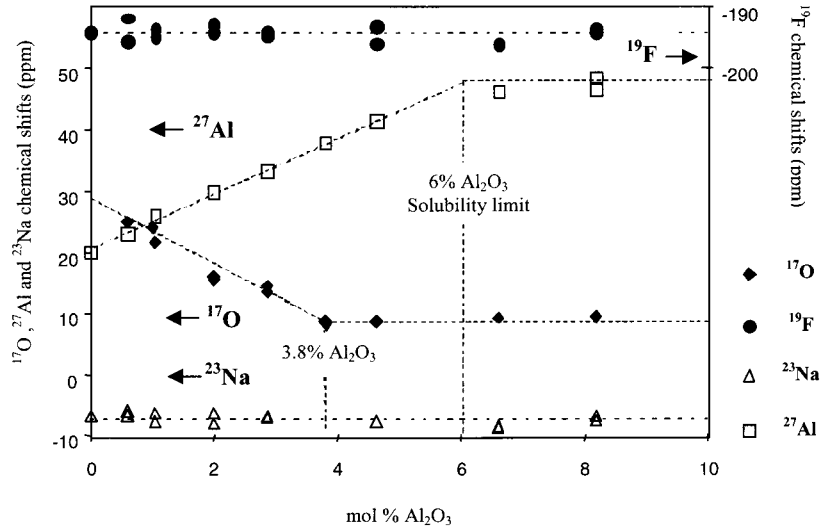

Figure 6. ^{17}O, ^{27}Al, ^{19}F, ^{23}Na chemical shifts evolution vs amount of alumina in cryolite (1000 °C).

From these relations and the experimental chemical shifts, it is possible to calculate the fractions of each oxyfluoride species over the whole range of alumina additions (Figure 7).

The interpretation of the ^{27}Al chemical shifts evolution is rather more complex because of the presence of fluoroaluminates species (AlF_x) in addition to the oxyfluorides. We assume in a first approach that the relative proportions of the AlF_x species are not modified by alumina additions in molten cryolite. We

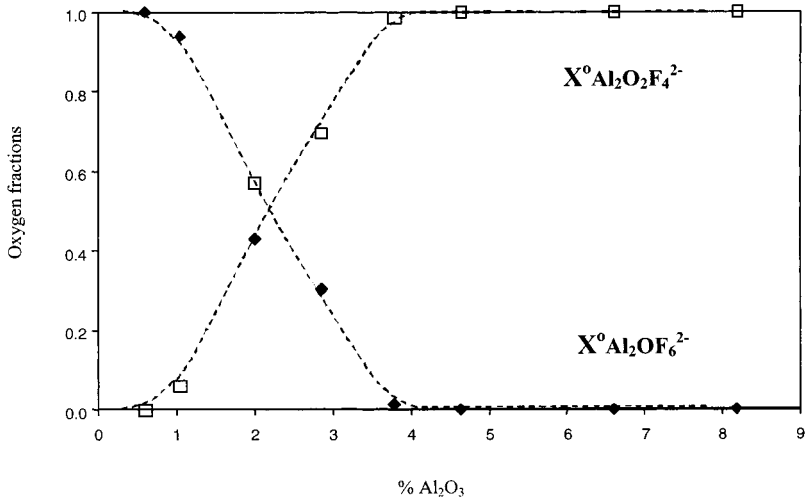

Figure 7. Evolution of oxygen fractions included in the oxyfluoro-aluminate species and directly calculated from the ^{17}O chemical shifts at 1000 °C.

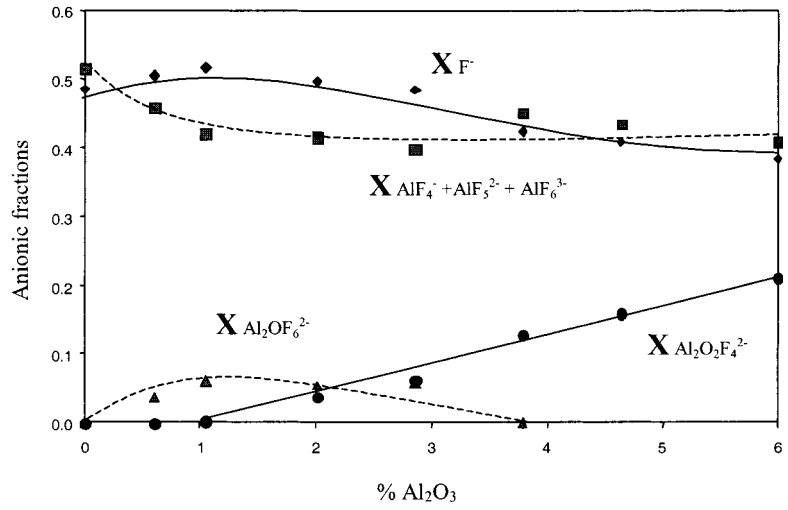

Figure 8. Anionic fractions of the different species in the molten cryolite alumina mixtures.

can then express the ^{27}Al chemical shift as

$$\delta(\mathrm{Al}) = X^{\mathrm{Al}}_{Al_2O_2F_4^{2-}}.\delta^{\mathrm{Al}}_{Al_2O_2F_4^{2-}} + X^{\mathrm{Al}}_{Al_2OF_6^{2-}}.\delta^{\mathrm{Al}}_{Al_2OF_6^{2-}} + X^{\mathrm{Al}}_{\mathrm{AlFx}}.\delta^{\mathrm{Al}}_{Na_3AlF_6} \quad (3)$$

with

$$X^{\mathrm{Al}}_{Al_2O_2F_4^{2-}} + X^{\mathrm{Al}}_{Al_2OF_6^{2-}} + X^{\mathrm{Al}}_{\mathrm{AlFx}} = 1 \quad (4)$$

and thus propose for the ^{27}Al of the two different oxyfluoride species:

$$\delta^{\mathrm{Al}}_{Al_2OF_6^{2-}} = 50 \pm 0.5 \text{ ppm and } \delta^{\mathrm{Al}}_{Al_2O_2F_4^{2-}} = 58.5 \pm 0.5 \text{ ppm}$$

For the NMR point of view, the local configuration around the aluminum atom in each of the two anions $Al_2OF_6^{2-}$ and $Al_2O_2F_4^{2-}$ can be described as a tetrahedral environment, respectively, $AlOF_3$ and AlO_2F_2. Compared to the two "extreme" AlO_4 (δ = 80 ppm) and AlF_4 (δ = 38 ppm), the two ^{27}Al chemical shifts values extracted experimentally are clearly intermediate between, and a difference of ≈10 ppm signs the substitution of one fluorine by one oxygen atom in the first coordination sphere of aluminum.

The evolution of ^{17}O and ^{27}Al chemical shifts over the whole domain of alumina addition, from a very low amount to above the saturation, allows us to describe the evolution of the atomic fraction of each nuclei and to deduce the anionic fraction of the different species present in the melt (Figure 8). The fraction of free fluorine slightly decreases over the whole range of composition. The global fraction of fluorine inside the fluoro-aluminate species decreases with increasing the alumina content, but keeps highly majority.

4. Conclusion

High-temperature NMR study of melts in $NaF-AlF_3$ and $NaF-AlF_3-Al_2O_3$ systems, by means of selective observation of the different nuclei involved in these systems: ^{27}Al, ^{23}Na, ^{19}F, and ^{17}O, provides a powerful tool for the structural description of such complex liquids.

In the binary $NaF-AlF_3$, the chemical shifts evolutions coincide rather well with the existence of AlF_4^-, AlF_5^{2-}, and AlF_6^{3-} complexes, with an averaged coordination of 5 for aluminum between cryolite and chiolite compositions, i.e., for $0.25 < X°(AlF_3) < 0.38$.

^{17}O NMR gives a selective view of the alumina dissolution in molten cryolite, because of its direct signature of the oxyfluoride complexes. From the variations of the ^{17}O chemical shift it is necessary to consider at least two different oxyfluorinated species: $Al_2OF_6^{2-}$, at low alumina content, and $Al_2O_2F_4^{2-}$, that becomes the major species for higher amounts of alumina.

Starting from simple assumptions, we have calculated the atomic fractions of oxygen present inside the different species. The combination of the different information given by the whole set of nuclei allows us to determine the anionic fractions of each species present in the melt and their evolution with alumina additions.

Acknowledgment. Pechiney is gratefully acknowledged for a doctoral fellowship to one of the authors (V.L.) and for financial support. Financial support from EEC ARI contract no. HPRICT-1999-00042, CNRS and Région Centre is also acknowledged. B. Gilbert and E. Robert are thanked for helpful discussions.

References and Notes

(1) Grojtheim, K.; Krohn, C.; Malinovsky, M.; Matiasovsky, K.; Thonstad, J. Aluminium electrolysis—Fundamentals of the Hall-Heroult process; 2nd ed.; Aluminium-Verlag: Düsseldorf; 1982.
(2) Gilbert, B.; Materne, T. *Appl. Spectrosc.* **1990**, *44* (2), 299−305.
(3) Robert, E.; Olsen, J. E.; Gilbert, B.; Østvold, T. *Acta Chem. Scand.* **1997**, *51*, 379−386.
(4) Robert, E.; Olsen, J. E.; Danek, V.; Tixhon, E.; Østvold, T.; Gilbert, B. *J. Phys. Chem. B* **1997**, *101*, 9447−9457.
(5) Stebbins, J.; Farnan, I.; Dando, N.; Tzeng, S.-Y. *J. Am. Ceram. Soc*. **1992**, *75*, 3001−3006.
(6) Lacassagne, V. Ph.D. Thesis, Orléans, France, 1998.
(7) Robert, E.; Lacassagne, V.; Bessada, C.; Massiot, D.; Gilbert B.; Coutures J.-P. *Inorg. Chem.* **1999**, *38*, 214−217.
(8) Bessada, C.; Lacassagne, V.; Massiot, D.; Florian, P.; Coutures, J.-P.; Robert, E.; Gilbert, B. *Z. Naturforsch*. **1999**, *54a*, 162−166.
(9) Xiang, F. N.; Kvande, H. *Acta Chem. Scand*. **1986**, *A 40*, 622−630.
(10) Dewing, E. W. *Metall. Trans. B* **1972**, *3*, 495−501.
(11) Dewing, E. W.; Thonstad, J. *Metall. Trans. B* **1997**, *28B*, 1089−1093.
(12) Holm, J. L. *Inorg. Chem*. **1972**, *12* (9), 2062−2065.
(13) Holm, J. L. *High Temp. Sci.* **1974**, *6*, 16−36.
(14) Sterten, A. *Electrochem. Acta* **1980**, *25*, 1673−1677.
(15) Danek, V.; Ostvold T. *Acta Chem. Scand*. **1995**, *49*, 411−416.
(16) Belashchenko, D. K.; Unikel, I. A. *Inorg. Chem.* **1997**, *333* (11), 1168−1172.
(17) Liska, M.; Perichta, P.; Turi Nagy, L. *J. Non Cryst. Solids* **1995**, *192 & 193*, 309−311.
(18) Akdeniz, Z.; Tosi, M. P. *Philos. Mag. B* **1991**, *2*, 167−179.
(19) Bouyer, F.; Picard, G.; Legendre, J.-J. *J. Chem. Inf. Comput. Sci.* **1995,** *4*, 684−693.
(20) Picard, G.; Bouyer, F.; Leroy, M.; Bertaud, Y.; Bouvet, S. *J. Mol. Struct. (THEOCHEM)* **1996**, *368*, 67−80.
(21) Castiglione M. J.; Ribeiro, M. C. C.; Wilson M.; Madden P. *Z. Naturforsch*. **1999**, *54a*, 605−610.
(22) Akdeniz, Z.; Ciçek, Z.; Tosi, M. P. *Chem. Phys. Lett*. **1999**, *308*, 479−485.
(23) Muller, D.; Bentrup, U. *Z. Anorg. Allg. Chem.* **1989**, *575*, 17−25 (in German).
(24) Dirken, P. J.; Jansen, J. B. H.; Schuiling, R. D. *Am. Mineral*. **1992**, *77*, 718−724.
(25) Spearing, D. R.; Stebbins, J. F.; Farnan, I. *Phys. Chem. Miner*. **1994**, *21*, 373−386.
(26) Kohn, S. C.; Dupree, R.; Mortuza, M. G.; Henderson, C. M. B. *Am. Mineral*. **1991**, *76*, 309−321.
(27) Smith, M. E.; Van Eck, E. R. H. *Prog. Nucl. Magn. Reson. Spectrosc*. **1999**, *34*, 159−201.
(28) Herron, N.; Thorn, D. L.; Harlow, R. L.; Davidson, F. *J. Am. Chem. Soc*. **1993**, *115*, 3028−3029.
(29) Lacassagne, V.; Bessada, C.; Ollivier, B.; Massiot, D.; Coutures, J.-P *C. R. Acad. Sci.* **1997**, *IIb*, 91−98.
(30) Walter, T. H.; Oldfield, E. **1989**, *93*, 6744−6751.
(31) Bastow, T. J.; Stuart, S. N. *Chem. Phys*. **1990**, *143*, 459−467.
(32) Stebbins, J. F. *Miner. Phys. Crystallogr*. **1995**, 303−331.
(33) Bonafous, L.; Bessada, C.; Massiot, D.; Coutures, J.-P.; Lerolland B.; Colombet, P. *Nuclear Magnetic Spectroscopic of Cement-Based Materials*; Colombet, P., Grimmer, A. R., Zanni, H., Sozzani, P., Eds.; Springer-Verlag, New York, 1998; pp 47−55.
(34) Massiot, D.; Trumeau, D.; Touzo, B.; Franan, I.; Rifflet, J. C.; Douy, A.; Coutures, J. P. *J. Phys. Chem.* **1995**, *99*, 16455−16459.
(35) Bonafous, L.; Ollivier, B.; Auger, Y.; Chaudret, H.; Bessada, C.; Massiot, D.; Farnan, I.; Coutures, J.-P. *J. Chim. Phys.* **1995**, *92*, 1867−1870.
(36) Du, L.-S.; Samoson, A.; Tuhem, T.; Grey, C. P. *Chem. Mater*. **2000**, *12*, 3611−3616.